Modern Physics Letters B
Vol. 34, No. 15 (2020) 2050159 (14 pages)

DOI: 10.1142/S0217984920501596

World Scientific
www.worldscientific.com

Multi-dimensional complex phase transition model by catastrophe theory developing Kolmogorov turbulence theory

Zhuo Zhou*, Jiu Hui Wu*,¶, Xiao Liang†,‖, Mei Lin‡, Xiao Yang Yuan§ and Yun Lei Wang*

*School of Mechanical Engineering and State Key Laboratory
for Strength and Vibration of Mechanical Structure,
Xi'an Jiaotong University, Xi'an, Shanxi 710049, China
†School of Mechanical Engineering, Xiangtan University, Xiangtan 411105, China
‡School of Energy and Power Engineering,
Xi'an Jiaotong University, Xi'an 710049, China
§Key Laboratory of Education Ministry for Modem Design and Rotor-Bearing System,
Xi'an Jiaotong University, Xi'an 710049, China
¶ejhwu@mail.xjtu.edu.cn
‖liangxiaoclh@126.com

Received 6 June 2019
Revised 25 November 2019
Accepted 5 December 2019
Published 4 March 2020

In this paper, a novel multi-dimensional complex non-equilibrium phase transition model is put forward to describe quantitatively the physical development process of turbulence and develop the Kolmogorov turbulence theory from the catastrophe theory, in which the well-known $-5/3$ power law is only a special case in this paper proving the accuracy of our methods. Catastrophe theory is a highly generalized mathematical tool that summarizes the laws of non-equilibrium phase transition. Every control variable in catastrophe theory could be skillfully expanded into multi-parameter multiplication with different indices and the relationship among these characteristic indices can be determined by dimensionless analysis. Thus, the state variables can be expressed quantitatively with multiple parameters, and the multi-dimensional non-equilibrium phase transition theory is established. As an example, by adopting the folding catastrophe model, we strictly derive out the quantitative relationship between energy and wave number with respect to a new scale index α to quantitative study the whole process of the laminar flow to turbulence, in which α varies from -2 to $-6/5$ corresponding to energy containing range and $\alpha = -9/5$ to energy containing scale where $-10/9$ power law is deduced, and at $\alpha = -6/5$ the $-5/3$ law of Kolmogorov turbulence theory is obtained, and fully developed turbulence phase starts at $\alpha = -2/3$ giving -3 law. Furthermore, this theory presented is verified by our wind tunnel experiments. This novel non-equilibrium phase transition methods cannot only provide a new insight into the turbulence model, but also be applied to other non-equilibrium phase transitions.

Keywords: Non-equilibrium phase transition; turbulence; power law; wind tunnel experiment.

¶Corresponding author.

1. Introduction

The non-equilibrium phase transition in all the applied sciences (e.g. Physics, Mechanics, Chemistry, etc.) is of great significance and importance. Turbulence defined as the chaotic behavior of fluid flows is ubiquitous in the oceans, atmosphere and the stares, and also occurs in a wide variety of engineering applications, from coffee mixed with milk to the flow of air around rockets and airplanes.[1–6] Up to date, the turbulent fluids have not been really analyzed mathematically satisfactorily.[7] The one striking success in turbulence research is the phenomenological picture introduced by Kolmogorov in 1941.[8,9] The two hypotheses in Kolmogorov turbulence theory are considered to be the most important contributions to predict the properties of fluid flow which indicate that the variables for the development of turbulence are the viscosity $v(\mathrm{m}^2/\mathrm{s})$, the mean dissipation rate $\varepsilon(\mathrm{m}^2/\mathrm{s}^{-3})$, and the scale $l(\mathrm{m})$ defined as the reciprocal of wave number $k(\mathrm{m}^{-1})$. By dimensionless argument, the second hypothesis implies the universal form in the inertial subrange for large wavenumbers as $E_{kk} = C_k\varepsilon^{2/3}k^{-5/3}$, where C_k is the Kolmogorov constant, and E_{kk} means the energy spectrum density.[9–11] It has been verified experimentally that the energy spectrum density in the inertial sub-range obeys the $-5/3$ law.[11–13]

In order to quantitatively study the whole process of the laminar flow to turbulence, the catastrophe theory with dimensionless analysis is applied in this paper. The catastrophe is theory advanced by Thom who proved that all kinds of catastrophe defining as the transition of the equilibrium state of a system in nature have only seven basic types.[14,15] The specific form of catastrophe model depends on the number of state variables and control parameters in the system. When the state variable is only one, the simplest catastrophe model is fold, and the more complicated models are known as cusp, swallow tail or butterfly.[16,17]

2. The Multi-Dimensional Complex Phase Transition Model by the Quantitative Catastrophe Approach

Considering that the fluid flow process only has two phases of laminar flow and fully developed turbulence, the simplest fold catastrophe model is adopted here, whose potential function is

$$V(x) = x^3 + tx \tag{1}$$

where t denotes the control variable, x is the state variable. The corresponding equilibrium curve is

$$V'(x) = 3x^2 + t \tag{2}$$

and the set of degenerate critical points of V (i.e. the critical points or the singularity set S) is given by

$$V''(x) = 6x = 0. \tag{3}$$

The potential function $V(x)$ of the fold catastrophe theory ($t < 0$) defined as the migration of equilibrium state is shown in Fig. 1(a), with P_1 (unstable equilibrium

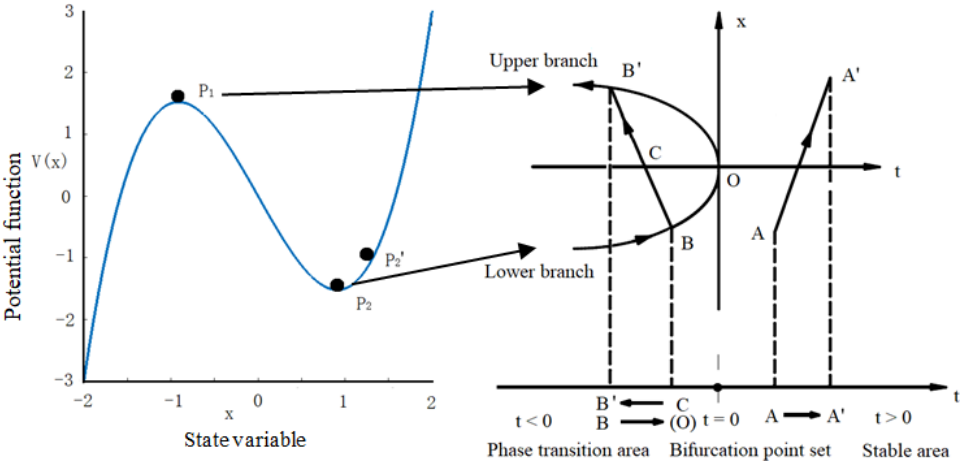

Fig. 1. (Color online) The fold catastrophe model (a) potential function ($t < 0$) and (b) the equilibrium curve of one-dimensional control variable.

state) and P_2 (stable equilibrium state), which correspond to the upper branch and lower branch of the equilibrium curve $V'(x)$ in Fig. 1(b), respectively. The P_1 point is an unstable equilibrium state. When external factors change at P_1, the equilibrium state of the system will be broken, and it is difficult for the system to return to equilibrium state. The P_2 is the stable equilibrium state of the system. As an example, the fluid flow includes unstable equilibrium state (laminar flow) and stable equilibrium state (fully developed turbulence). The laminar flow is easily broken under the influence of active factors such as velocity, external driving force at the point of P_1. The fully developed turbulence is at the point of P_2. The whole process of the laminar flow to turbulence is from the unstable equilibrium state to the stable by the external control variables.

As shown in Fig. 1(b), the bifurcation point set ($t = 0$) obtained by combining $V'' = 0$ with $V' = 0$ divides the control variable into ($t > 0$) and ($t \leq 0$) regions. When control variable $t > 0$, there is no real solution of Eq. (2), and the $V(x)$ has no critical points with the stable state transition (A–A'). In this process, the phase transition will not occur. When $t \leq 0$, Eq. (2) has real solutions, and $V(x)$ has two critical branches in Fig. 1(b), where the upper branch represents the unstable equilibrium state of the system (corresponding to the point P_1 in Fig. 1(a)) and the lower branch represents the stable equilibrium state (corresponding to the point P_2 in Fig. 1(a)). When the system moves from the lower branch crossing the upper branch (B–C–B') in the region of $t < 0$, there is a sudden accumulation and release of energy, the system state will suddenly change. On the other hand, when the system moves continuously (B–O–B'), the system passes through the bifurcation point set ($t = 0$) and the system gradually finishes the migration of equilibrium state.

Therefore, the folding catastrophe model can describe the two-phase transformation process by considering only one parameter t. In general, this two-phase transition process may be affected by many factors such as input energy, temperature, pressure and so on. Thus, according to the form of the well-known turbulence $-5/3$ power law ($E_{kk} = C_k\varepsilon^{2/3}k^{-5/3}$), the control variable is proposed in the form of $t = At_1^{\alpha_1}t_2^{\alpha_2}t_3^{\alpha_3}\ldots t_n^{\alpha_n}$, where $t_1, t_2, \ldots$ and t_n are the related different active parameters, and $\alpha_1, \alpha_2, \ldots$ and α_n are the corresponding scaling indices. The multi-dimensional fold catastrophe model combining with fold catastrophe model Eq. (1) can be expressed as

$$x^2 + At_1^{\alpha_1}t_2^{\alpha_2}t_3^{\alpha_3}\ldots t_n^{\alpha_n} = 0\,, \tag{4}$$

where A is a constant less than 0, and the relationship among the indices $\alpha_1, \alpha_2, \ldots$ and α_n can be further determined by the non-dimensional analysis in the following. In which, the n dimensions of the exponents of $t_1^{\alpha_1}t_2^{\alpha_2}t_3^{\alpha_3}, \ldots, t_n^{\alpha_n}$ can be reduced to the $(n-m+1)$ dimension with $t_1^{\alpha_1(\alpha_m,\ldots,\alpha_n)}t_2^{\alpha_2(\alpha_m,\ldots,\alpha_n)}t_3^{\alpha_3(\alpha_m,\ldots,\alpha_n)}\ldots t_m^{\alpha_m}\ldots t_n^{\alpha_n}$ by the m related unit dimensions of parameters $t_1, t_2, \ldots, t_n$. Then, the quantitative relationship between the phases of the system can be obtained by equilibrium curve or surface equation ($V' = 0$) and the singularity set S or critical points equation ($V'' = 0$). Finally, we can get different indexes α_i ($i = 1, 2, \ldots, n$) values by solving the extremum of the potential function, which can describe the quantitative relationship of each phase in the system.

For a simple, multi-dimensional model with two control variables t_1 and t_2, the equilibrium surface and bifurcation point set are shown in Fig. 2 when $A < 0$. The equilibrium surface with two-dimensional control variables also includes the bifurcation point set and the equilibrium state point set as the equilibrium curve of

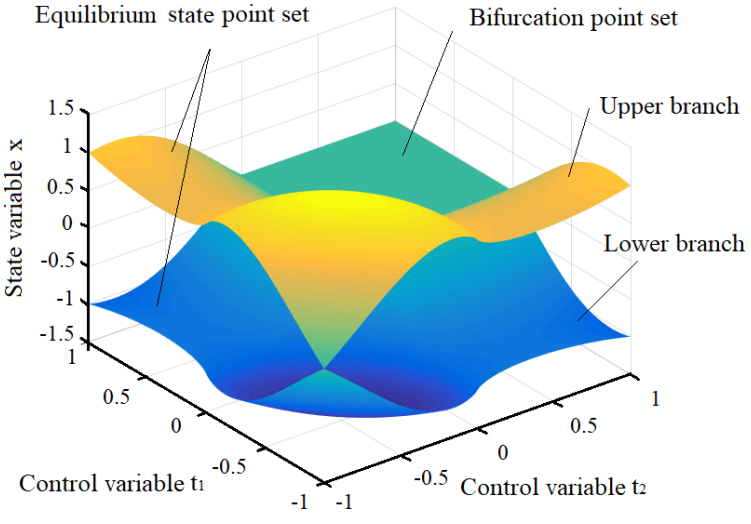

Fig. 2. (Color online) The equilibrium surface of two-dimensional control variables.

one-dimensional control variable mentioned above. So, by extending the dimension number of parameters of the control variable t to $t = f(t_1, t_2)$, it can be obtained how the two parameters affect the phase transition of the system.

3. Improved Kolmogorov's Turbulence Theory by the Multi-Dimensional Complex Phase Transition Model

As described in Kolmogorov's turbulence theory, in the inertial subrange, $\eta \ll 1/k \ll L$, the viscous effect is not important, and the motion of fluid is mainly determined by the inertial force. It is only related to its scale $1/k$ and energy dissipation rate ε (According to Kolmogorov's second universality assumption). Within the Kolmogorov scales and Taylor scales, the viscous dissipation is approximately equivalent to the kinematic viscosity (According to Kolmogorov's first universality assumption). In addition, the physicists use the wave number $k(L^{-1})$ to study the turbulent phenomenology, which became the main tool for Kolmogorov's energy cascade chain.[1,9,18–20] Therefore, the k can be selected to be the state variable, and the viscosity $v(L^2T^{-1})$, the mean energy dissipation rate $\varepsilon(L^2T^{-3})$, and energy spectrum density $E_k(L^3T^{-2})$ are selected as control variables.[9,10,21–23] The t is in the multidimensional function form based on non-equilibrium phase transition theory[2,9–13]

$$t = 3A\varepsilon^{\alpha_1}\nu^{\alpha_2}E^{\alpha}\,, \tag{5}$$

where A is a constant less than 0, and $\alpha_1, \alpha_2, \alpha$ denote time scaling indices. As a new physical phenomenon, α has been the dimension of time describing the formation process of turbulence. Meanwhile, the kinematic viscosity v can describe the Reynolds number defined as $R = LV/\nu$.[9] Moreover, the dimension of Eqs. (5) and (6) is shown in Table 1.

Table 1. The power exponents relation.

	α_1	$\alpha_2(\varepsilon)$	$\alpha(E_k)$	t
L	2	2	3	-2
T	-1	-3	-2	0

By the dimensionless analysis, the dimension satisfies the relation $\begin{cases} 2\alpha_1 + 2\alpha_2 + 3\alpha = -2 \\ -\alpha_1 - 3\alpha_2 - 2\alpha = 0 \end{cases}$ and Eq. (6) is derived by Eqs. (2) and (5).

$$k^2 + A\nu^{\frac{-6-5\alpha}{4}}\varepsilon^{\frac{2-\alpha}{4}}E_k^{\alpha} = 0. \tag{6}$$

The dimensions of identities of Eq. (6) are always balanced and established for any wave numbers k in the turbulence formation process analyzed by the theory which can quantitatively describe the Kolmogorov energy cascade described by any $k(n)$. Furthermore, the formula of energy spectrum E_k is solved by Eq. (6):

$$E_k = -A^{-\frac{1}{\alpha}}\varepsilon^{\frac{\alpha-2}{4\alpha}}\nu^{\frac{5\alpha+6}{4\alpha}}k^{\frac{2}{\alpha}}. \tag{7}$$

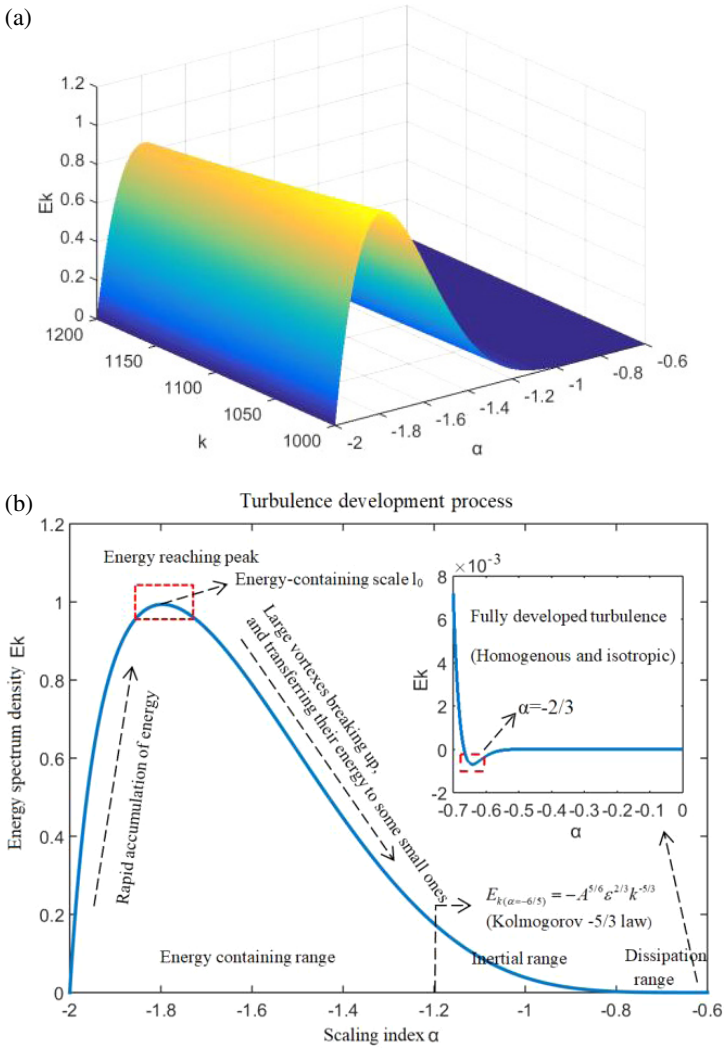

Fig. 3. (Color online) (a) Energy spectrum density E_k as a function of the index α and the k and (b) energy spectrum density E_k as a function of the index α.

Thus, we derive the quantitative expression between energy E_k and Kolmogorov cascade k theoretically and physically, which can quantitatively calculate the energy difference dissipated by viscous motion between the $k(n+1)$ and $k(n)$, where n is the level of turbulent energy cascade chain.

Figure 3 shows the energy spectrum density E_k by Eqs. (6) and (7) with index α and k. The turbulent development process includes five special stages from Fig. 3, which are $\alpha = -2$, $\alpha = -9/5$, $\alpha = -6/5$ (obtained from $\frac{\partial^2 E}{\partial \nu^2} = 0$ described as the set of degenerate critical points), $\alpha = -2/3$ (obtained from $\frac{\partial^2 E}{\partial \varepsilon^2} = 0$ described as the set of degenerate critical points), and $\alpha = 0$. $\alpha = -2$ is the starting point of the

change in turbulent kinetic energy. The range near $\alpha = -9/5$ is energy containing range in which the range $-2 \leq \alpha \leq -9/5$ is laminar-turbulence transition stage for low Reynolds. In this region, fluid energy increases rapidly, mainly affected by the continuous input of external kinetic energy or the increasing Reynolds number. The maximum energy is generated at $\alpha = -9/5$ reaching its peak after numerical calculation corresponding to the energy-containing scale l_0, and its reciprocal is the energy-containing wave number $k_0 = 1/l_0$ from Fig. 3. The maximum energy peak is the maximum value of spectrum density in the turbulence formation process in which turbulence pulsation takes up almost all turbulent kinetic energy, which transfers energy through inertia, and the dissipation of turbulent kinetic energy can be ignored. Then, these large eddies are unstable and easily break up, and transfer their energy to some small eddies. In the range $-9/5 \leq \alpha \leq -6/5$, energy is transferred through inertia. Then, the range near $\alpha = -6/5$ is the inertial subrange, where the vortex receives the energy from the large-scale pulsation without dissipating, and then passes the energy to the smaller-scale vortex. In this range, Kolmogorov's $-5/3$ law is obtained and analyzed in Eq. (10). When $-1 \leq \alpha \leq -2/3$, these small eddies undergoing a similar break-up, transfer their pulsation energy to yet smaller ones. Finally, the pulsation energy is completely dissipated by viscous motion at $\alpha = -2/3$, where turbulence develops into fully developed turbulence, at the same time, the fluid system reaches dynamic and statistical equilibrium. The $\alpha = -2/3$ is the second partial derivative of E with respect ε is zero ($\frac{\partial^2 E}{\partial \varepsilon^2} = 0$ described as singularity set or critical points in the catastrophe theory) where only the turbulent kinetic energy is dissipated, and the energy transmission is almost zero.

So, $\alpha = -2$ is the unstable equilibrium state in which the state of the system can easily be broken. $\alpha = -2/3$ is the stable equilibrium state. According to Kolmogorov cascade theory, the energy of the n stage vortexes obtained from the $(n-1)$ stage and passed to the $(n+1)$ stage vortexes can be quantified in almost all scales at the entire phase transition. The description of turbulence variation in Fig. 3 is consistent with Poisson distributions in document,[27] and the lognormal scale distributions of turbulence in Fig. 4 will be verified in experiments.

Thus, the range near $\alpha = -9/5$ is energy containing range in which $\alpha = -9/5$ is the maximum energy peak corresponding to the energy-containing scale l_0, the area near $\alpha = -6/5$ is the turbulence development range (transition region), and the area near $\alpha = -2/3$ is the fully developed turbulence stage. Therefore, the energy spectrum density for some special transition stages, $\alpha = -2$, $\alpha = -9/5$, $\alpha = -6/5$, $\alpha = -2/3$ can be obtained by solving Eq.(7).

$$E_{k(\alpha=-2)} = -A^{1/2}\varepsilon^{1/2}\nu^{1/2}k^{-1}\,, \tag{8}$$

$$E_{k(\alpha=-9/5)} = -A^{5/9}\varepsilon^{19/36}\nu^{5/12}k^{-10/9}\,, \tag{9}$$

$$E_{k(\alpha=-6/5)} = -A^{5/6}\varepsilon^{2/3}k^{-5/3}\,, \tag{10}$$

$$E_{k(\alpha=-2/3)} = -A^{3/2}\varepsilon^{1}\nu^{-1}k^{-3}\,. \tag{11}$$

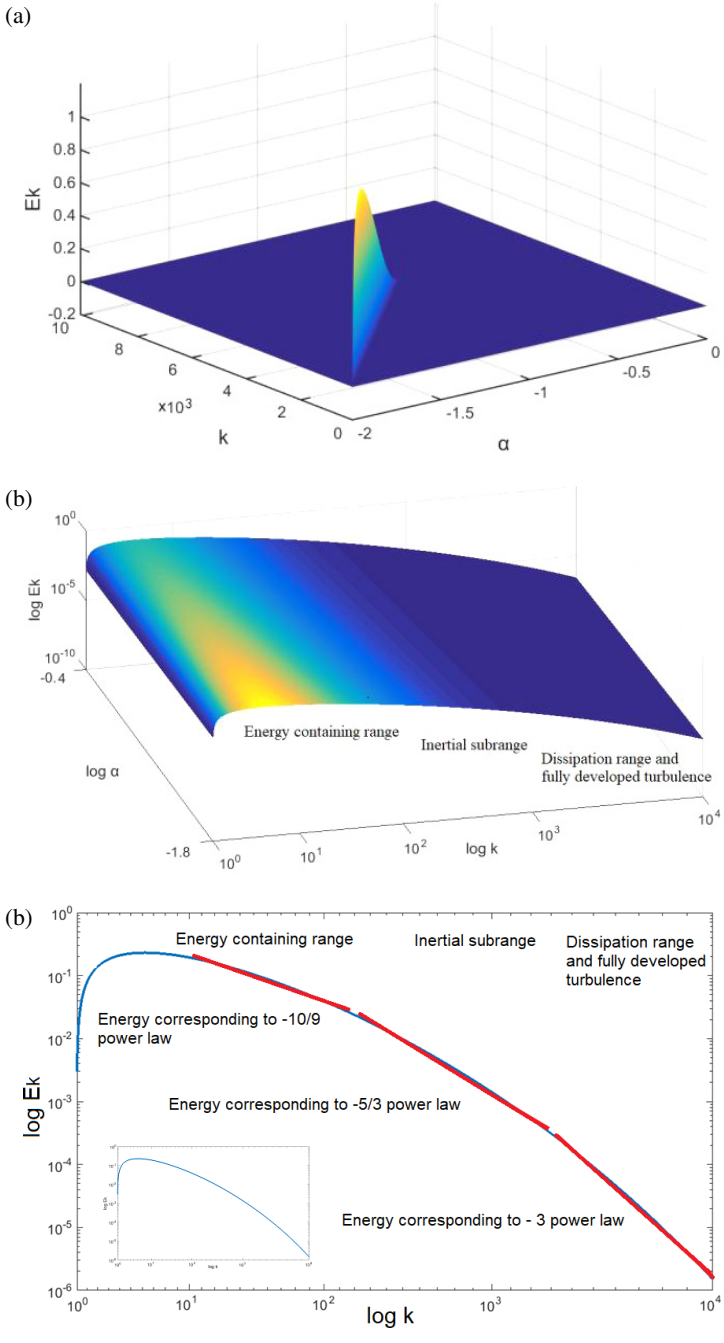

Fig. 4. (Color online) (a) Three-dimensional energy spectrum density with the wave number and scaling indices, (b) three-dimensional logarithmic map of energy spectrum density in the turbulent development stage and (c) two-dimensional logarithmic map of energy spectrum density with wave number.

Equation (8) shows that the energy begins to accumulate from $\alpha = -2$ so that the unstable equilibrium phase is broken, and the flow line begins to be confused. Equation (9) shows that the cumulative pulsation energy attains the maximum value at $\alpha = -5/9$ in the energy containing range, as the turbulence-onset, where the energy spectrum density E_k is in direct proportion to the $-10/9$ of $k(k^{-10/9})$. Importantly, Eq. (10) is exactly the same as $E_{kk} = C_k\varepsilon^{2/3}k^{-5/3}$ for Kolmogorov's second universality assumption. So, the fact that the energy spectrum density E_k is in direct proportion to the $-5/3$ power law of the k corresponding to Kolmogorov's turbulence theory just as a special case in the multi-dimensional complex phase transition theory, verifies the multi-dimensional complex phase transition theory presented in this paper. Equation (11) is the fluid flow for the dissipation and the fully developed turbulence range near $\alpha = -2/3$, while viscous motion completely converts turbulent energy into heat energy. The energy spectrum density E_k is in direct proportion to the -3 of $k(k^{-3})$. Equation (11) corresponds to Kolmogorov's first universality assumption, and gives the expression of parameters and the index of the k for the fully developed turbulence.

As can be seen from Fig. 1, the potential function has two different equilibrium states, representing the laminar and turbulent states. Then, every control variable in catastrophe theory could be skillfully expanded into multi-parameter multiplication with different indices α defined as a time scale factor. In the process of fluid flow, the energy increases with the wave number and time in Fig. 4(a). Thus, taking the logarithm of the energy spectral density, the power law corresponding to the energy can be obtained from Figs. 4(b) and 4(c). The energy spectrum density for large-scale wave corresponds to $-10/9$ power law in energy containing range. The energy spectrum density corresponds to $-5/3$ power law in the inertial subrange. The energy spectrum density for small scale wave corresponds to -3 power law in the fully developed turbulence range.

Although Kolmogorov only gives the quantitative expression of energy in the inertial range, his qualitative analysis of the flow based on three important assumptions still provides a guideline to study the quantitative question for fluid flow. This multi-dimensional phase transition theory cannot only explain and develop the Kolmogorov theory theoretically, but also can describe the whole phase transition process of fluid movement and study the quantitative relationship of each parameter.

4. The Analysis and Feasibility Verification Using *T*-Tube Wind Tunnel

To verify the variation for the energy spectrum of this new method in the turbulence phase transition, we have conducted experiments in the T-tube connection system which are very common in mechanical power system, such as gas and oil transmission systems, high-speed train ventilation systems, etc. Figure 5 shows were

simplified experimental wind tunnel platform constructed in the Xi'an Jiao Tong University.

The T channel is made of plexiglass, whose main passageway and branch are connected with the wind tunnel and small fan, respectively. We can control the flow of the main road by adjusting the frequency of the fan. The length of the T-shaped tube channel is 143.3×161.7 mm^2, and the length of the rectangular section is 35.5D. The branch tube with a cross-section $D = 110$ mm is 14.2 D. In order to ensure that fluid is more likely to form turbulence in the T-wind tunnel, a 2.0 mm rod is fixed to the tunnel side at the main inlet in Fig. 5(a).

The coordinate origin is situated on the center of main interface and branch interface in Fig. 5(b). In the (x, y) plane, the ratio $R = u_b/u_c$ of the branching velocity of the bulk to the cross-velocity at the horizontal axis center is shown in Table 2. Measure the velocity component of the sum with an X-type hot wire

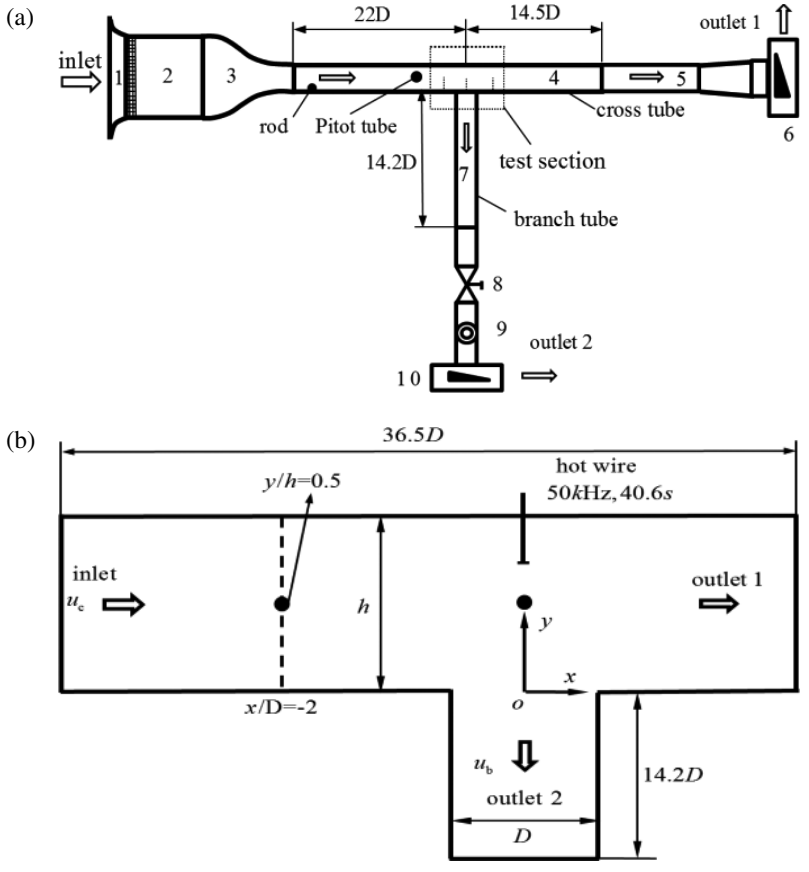

Fig. 5. Schematic diagram of the T-tube wind tunnel measurement (a) Experimental devices 1 — Entrance, 2 — Settling chamber, 3 — Contraction section; 4 — Cross duct, 5 — Connect section, 6 — Fan, 7 — Branch tube, 8 — Valve, 9 — Rotameter, 10 — Fan and (b) sketch of measurement points.

Table 2. Velocity design condition.

	u_b (m/s)	u_c (m/s)	R
1	30	3.9	0.13

Table 3. Design of measuring points.

Position	Distance from wall surface (mm)	Distance from T tube center (mm)
P_1	71.6	$-2D$
P_2	71.6	0

probe $-$TSI $1240-20$. The uncertainty of average cross-velocity measured by using hot wire probe method and the branching velocity measured by using glass rotor method are 1% and 4.3%, respectively. In consideration of the repeated testing, measurement points are determined as shown in Table 3. Then the P_1, P_2 velocities are collected for the time of 40.6 s in Table 3. The accuracy and procedures of the test method and data processing methods refer to document by Gessner, Elazhary and Soliman.[24–26]

The statistics for instantaneous velocity $u(t)$ is expressed as:

$$\langle u^m \rangle = \int_{-\infty}^{\infty} u^m p(u) du = \frac{1}{N} \sum_{i=1}^{N} m \geq 1\,, \tag{12}$$

where $p(u)$ represents the PDF for the instantaneous state of velocity $u(t)$, $\langle \cdot \rangle$ is the time-average velocity.

The PDF can be expressed as Eq. (13) when the random variable u' complies with probability distribution

$$p(u') = \frac{1}{\sqrt{2\pi\sigma^2}} \exp\left(-\frac{(u'-\mu)^2}{2\sigma^2}\right), \tag{13}$$

where σ denotes scale parameter and μ is position parameter. Furthermore, Eq. (14) is well known as the standard normal distribution or the Gaussian distribution if $\sigma = 1$, $\mu = 0$

$$p(u') = \frac{1}{\sqrt{2\pi}} \exp\left(-\frac{u'^2}{2}\right). \tag{14}$$

Other parameters are defined as follows: fluctuation velocity is $u' = u - \bar{u}$, time-average velocity is defined as that $\bar{u} = \frac{1}{N}\sum_{i=1}^{N} u_i$, Reynolds number is that $\mathrm{Re}_a = \frac{u_a h}{v}$, friction Reynolds number or Kármán number is defined as that $\mathrm{Re}_\tau = \frac{u_\tau h}{v}$, velocity ratio is that $R = \frac{u_b}{u_c}$ and bulk velocity is defined as that $u_a = \frac{1}{h}\int_0^h \bar{u}(y)dy$.

Turbulent flow can be seen as a superposition of vortexes for different scales. Since the instantaneous velocity can be regarded as the superimposition of the

average and pulsation velocity, the power spectrum density is defined as follows:

$$\int_0^\infty P(f)df = (\bar{u}')^2\,, \tag{15}$$

where sampling frequency is that $f = \frac{n}{N\Delta t}$, $n = 0, 1, 2, \ldots, N-1$, so power spectrum density is $P(w) = \frac{1}{N}|x(w)|^2 = \frac{1}{N}|\sum_{n=0}^{N-1} x(n)e^{-jwn}|^2$, the relationship between power spectrum density $P(w)$ and the energy spectrum density E is:

$$E = \frac{1}{2\pi}\int_{-\infty}^{+\infty} P(w)dw\,. \tag{16}$$

Using Welch method[27,28] and MATLAB software to calculate the power spectrum of the pulse velocity signal, and then study the law in logarithmic form.

Figure 6 shows the relation between the E_k and α for the T-tube wind tunnel experimental data at two positions where (a) $x/D = 0$, $y/L = 1/2$ (b) $x/D = -2$, $y/L = 1/2$ in the form of logarithm in ordinate and $f = kv/2\pi$, where k is the wave number, and v is the volume velocity of the fluid.

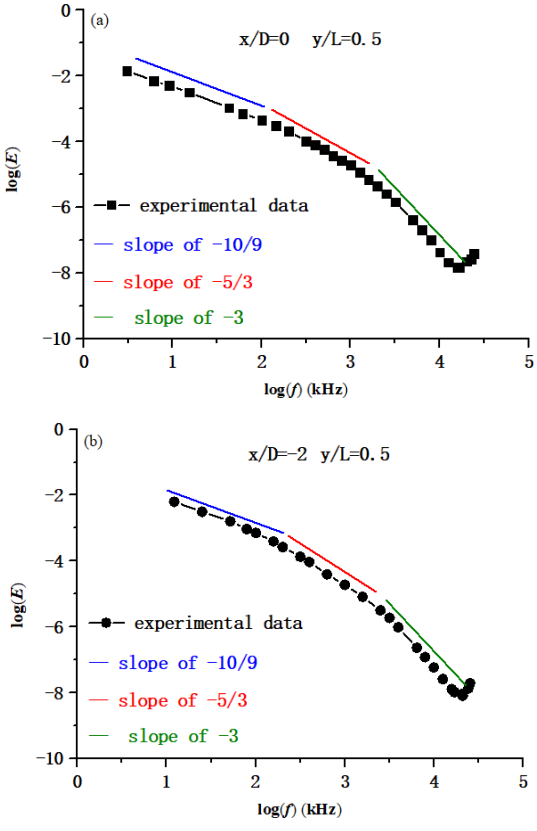

Fig. 6. (Color online) T-tube wind tunnel experimental data relationship between E and α in the form of logarithmic. (a) $x/D = 0$, $y/L = 1/2$ and (b) $x/D = -2$, $y/L = 1/2$.

The T-tube wind tunnel experimental data for low-frequency describe the change rules of small wave number — large-scale vortexes when turbulence starts, where energy spectrum density E_k is in direct proportion to the $-10/9$ of $k(k^{-10/9})$ (blue line in Fig. 6). The T-tube wind tunnel experimental data for medium frequency describe the law of variation of medium scale vortexes when turbulence develops, where E_k is proportional to the $-5/3$ of $k(k^{-5/3})$ (red line in Fig. 6). The T-tube wind tunnel experimental data for high frequency describe the change rules of large wave number-small scale vortexes in statistical equilibrium range, where the E_k is in direct proportion to the -3 of $k(k^{-3})$ (green line in Fig. 6).

This theory successfully predicts and indicates the quantitative relationship between the turbulence just occurring ($-10/9$ power law) and the energy dissipated completely by fluids' viscous occurring (-3 power law), respectively. Meanwhile, Kolmogorov's $-5/3$ power law is also found and is just a special case in our results. Furthermore, we theoretically and mathematically derive this turbulence model that can explain the whole phase transition process of turbulence quantitatively. The fact that Kolmogorov' $-5/3$ law for energy spectrum in the inertial range in our theory verifies our theory presented in this paper.

5. Conclusions

The multi-dimensional complex phase transition theory is proposed to develop the Kolmogorov turbulence theory. Through this multi-dimensional method, we quantitatively study the whole process of the laminar flow to turbulence. We conclude that the energy spectrum density E_k is in direct proportion to the $-10/9$ of $k(k^{-10/9})$ in the energy-containing range and $\alpha = -9/5$ corresponds to energy-containing scale l_0. In the inertial subrange, the E_k is in direct proportion to the $-5/3$ of $k(k^{-5/3})$, in the final period of isotropic turbulence, the E_k is in direct proportion to the -3 of $k(k^{-3})$.

Importantly, the fact that the E_k is in direct proportion to the $-5/3$ of $k(k^{-5/3})$ in the inertial subrange is only a special case in the whole process also verifying the correctness of multi-dimensional complex phase transition theory.

Acknowledgments

This work was supported by the National Natural Science Foundation of China (NSFC) under Grant Nos. 51376145 and 51675401.

References

1. J. I. Cardesa, A. Vela-Martín and J. Jiménez, *Science* **357** (2017) 782.
2. K. P. Iyer, J. Schumacher, K. R. Sreenivasan and P. K. Yeung, *Phys. Rev. Lett.* **121**(26) (2018) 264501.
3. M. C. Montoya, F. Nieto, A. J. Alvarez, S. Hernández, J. A. Jurado and R. Sanchez, *Eng. Appl. Comput. Fluid* **12**(1) (2018) 750.
4. L. L. Tian, N. Zhao, Y. L. Song and C. L. Zhu, *Mod. Phys. Lett. B* **32** (2018) 1840038.

5. A. Farhadi, A. Mayrhofer, M. Tritthart, M. Glas and H. Habersack, *Eng. Appl. Comput. Fluid* **12**(1) (2018) 216.
6. Z. Liang, S. Shan, X. Liu and Y. Wen, *Eng. Appl. Comput. Fluid* **11**(1) (2017) 225.
7. Z. Warhaft, *Proc. Natl. Acad. Sci. USA* **99** (2002) 3.
8. M. Nelkin, *Science* **255** (1992) 5044.
9. U. Frisch, *Turbulence: The Legacy of A. N. Kolmogorov* (Cambridge University Press, Cambridge, 1995).
10. J. H. Wu, Z. P. Hu and H. Zhou, *J. Appl. Phys.* **113**(19) (2013) 194905.
11. B. Sun, *Mod. Phys. Lett. B* **30**(23) (2016) 1650297.
12. P. M. Chesler, H. Liu and A. Adams, *Science* **341**(6144) (2013) 368.
13. J. Maurer, P. Tabeling and G. Zocchi, *Adv. Turbulence* **26** (1995) 31.
14. O. Raz, O. Pedatzur, N. Dudovich and B. D. Bruner, *Nat. Photonics* **6** (2012) 170.
15. B. Goodwin, *Nature* **309** (1984) 5963.
16. M. J. Bazin and P. T. Saunders, *Nature* **275** (1978) 5675.
17. H. Chilver, *Nature* **254** (1975) 5499.
18. A. N. Kolmogorov, *Dokl. Akad. Nauk SSSR* **31** (1941) 538.
19. H. Zhu and K. Cheng, *Mod. Phys. Lett. B* **23**(03) (2009) 513.
20. C. E. Leith, *Phys. Fluids* **10** (1967) 1409.
21. A. C. Poje, T. M. Ozgokmen, D. J. Bogucki and A. D. Kirwan, *Phys. Fluids* **29** (2017) 2.
22. A. N. Kolmogorov, *Dokl. Akad. Nauk SSSR* **32** (1941) 16.
23. J. I. Cardesa, A. Vela-Martín, S. Dong and J. Jiménez, *Phys. Fluids* **27** (2015) 11.
24. F. B. Gessner, J. K. Po and A. F. Emery, *Measurements of Developing Turbulent Flow in a Square Duct, Turbulent Shear Flows* 1, Vol. 119 (Springer, New York, 1979).
25. A. M. Elazhary and H. M. Soliman, *Int. J. Multiphas Flow* **42** (2012) 104.
26. Y. T. Yin, S. C. Lin and L. B. Wang, *Energies* **11** (2018) 864.
27. A. A. Masoudi and P. A. Anaraki, *Mod. Phys. Lett. B* **20**(20) (2006) 1247.
28. O. A. Jaiboon, B. Chalermsinsuwan, L. Mekasut and P. Piumsomboon, *Powder Technol.* **233** (2013) 215.